Molecular Microbiology (2007) **63**(2), 454–467
doi:10.1111/j.1365-2958.2006.05536.x
First published online 14 December 2006

Gliding motility and polarized slime secretion

Rosa Yu[†] and Dale Kaiser*
Departments of Biochemistry and of Developmental Biology, Stanford University School of Medicine Stanford, CA 94305, USA.

Summary

Myxococcus leaves a trail of slime on agar as it moves. A filament of slime can be seen attached to the end of a cell, but it is seen only at one end at any particular moment. To identify genes essential for A motility, transposon insertion mutations with defective A motility were studied. Fifteen of the 33 mutants had totally lost A motility. All these mutant cells had filaments of slime emerging from both ends, indicating that bipolar secretion prevents A motility. The remaining 18 A motility mutants, also produced by gene knockout, secreted slime only from one pole, but they swarmed at a lower rate than A^+ and are called 'partial' gliding mutants, or *pgl*. For each *pgl* mutant, the reduction in swarm expansion rate was directly proportional to the reduction in the coefficient of elasticotaxis. The *pgl* mutants have a normal reversal frequency and normal gliding speed when they move. But their probability of movement per unit time is lower than *pgl*$^+$ cells. Many of the *pgl* mutants are produced by transposon insertions in glycosyltransferase genes. It is proposed that these glycosyltransferases carry out the synthesis of a repeat unit polysaccharide that constitutes the slime.

Introduction

Many bacteria glide; they translocate across surfaces without the aid of flagella, and they cannot swim (Henrichsen, 1972). How is gliding propelled? Some bacteria glide by retracting polar type IV pili, as reviewed (Nudleman and Kaiser, 2004). Other gliders lack type IV pili: members of the cytophaga-flavobacterium group and the mycoplasms (for example, McBride, 2001). Moreover, mutants of *Myxococcus xanthus* that have lost their ability to produce type IV pili, and hence their S motility, continue to glide. They use what has been called adventurous or A motility, the subject of this report (Hodgkin and Kaiser, 1979a,b).

The molecular basis of A motility has long been sought. Observing trails of slime, Jahn suggested that myxobacteria might be propelled by slime secretion, but he questioned whether slime was capable of pushing cells along (Jahn, 1924). Hodgkin approached the problem by isolating mutants specifically deficient in A motile gliding as opposed to S motile gliding (Hodgkin and Kaiser, 1979a). When the amino acid sequences of A motility genes became available, they revealed many proteins: outer membrane lipoproteins (Rodriguez and Spormann, 1999), transport proteins, proteases and peptidases (Youderian *et al.*, 2003). But the ensemble of proteins failed to suggest a mechanism.

An electron microscopic examination of slime secretion associated with gliding was undertaken in *Phormidium*, a filamentous gliding cyanobacterium (Hoiczyk and Baumeister, 1998). Hoiczyk and Baumeister observed the extrusion of slime from junctional pore complexes in the cell wall, and correlated the rate of slime extrusion with the speed of movement of the cyanobacterial filaments. The junctional pore complexes were pore-shaped organelles embedded in the cell wall near the sites of slime extrusion (Hoiczyk and Baumeister, 1998). Recently, ribbons of an amorphous material, taken to be slime, were photographed emerging from the ends of *M. xanthus* cells (Wolgemuth *et al.*, 2002). Next to the cell, the ribbons were thin, while farther from the cell they coalesced into a single ribbon having the width of the cell (Wolgemuth *et al.*, 2002). Strikingly, the ribbons emerged uniquely from one pole of the cell; the other pole was devoid of ribbons.

A^+ cells (both A^+S^+ and A^+S^-) are found either depositing slime as they glide on agar, or gliding on a trail left by another cell (Wolgemuth *et al.*, 2002). A^+ gliding cells seem to prefer to follow a slime trail previously laid down than to lay a new trail (Burchard, 1982). Many examples of individual myxobacterial cells turning to follow a slime trail are shown in Reichenbach's time lapse movies (Reichenbach *et al.*, 1965). The deposition and the following of slime trails are independent of the presence or absence of pili or S motility in *M. xanthus* (Wolgemuth *et al.*, 2002). Burchard showed that *Myxococcus* can also follow the slime trails of other gliders like *Beggiatoa* and *Oscillatoria* (Burchard, 1982). Elasticotaxis denotes the ability of *Myxococcus* cells to orient their movement along lines of elastic stress in an agar gel that has been

Accepted 21 November, 2006. *For correspondence. E-mail kaiser@cmgm.stanford.edu; Tel. (+1) 650 723 6165; Fax (+1) 650 725 7739. [†]Present address: Osel Inc., 4008 Burton Drive, Santa Clara, CA 95054, USA.

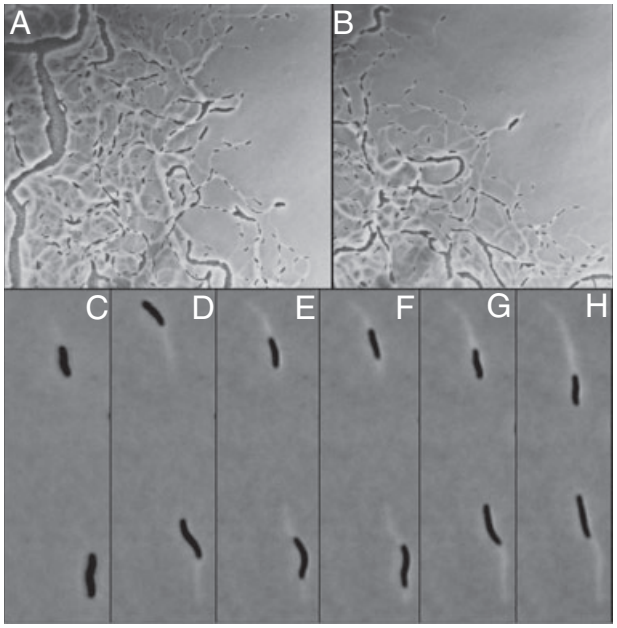

Fig. 1. *M. xanthus* lays down slime trails and follows them. Frames A and B show the swarm front of the A^+S^- strain DK10410 on agar photographed after 1 day at 32°C. Photographs taken with a Leitz 16×, phase contrast objective. Frames C–H show two cells of the A^+S^+ strain, DK1622, gliding on agarose. Photographs taken with a Nikon 40×, phase contrast objective by Dr Lars Jelsbak.

stretched or compressed (Stanier, 1942). Elasticotaxis is related to slime trails by the fact that it is restricted to A motile cells. Moreover, A motile cells display less elasticotaxis when they also exhibit S motility (Fontes and Kaiser, 1999).

In this report, we suggest that A motility, the following of slime trails, and elasticotaxis are different manifestations of the secretion, swelling and alignment of polymeric slime. In support of that suggestion, we report two new classes of mutants with defects in A motility. One class produces slime from both ends of the cell and is non-motile. The other class of gene knockout mutants diminishes A motility to different degrees, but does not abolish it.

Results

Isolating A motility mutants

To explore the connection between A motility and slime secretion, we isolated a random set of A motility mutants and examined their ability to secrete slime. Two A^+S^- strains were exposed to the Himar transposon, and drug-resistant strains that formed small colonies were isolated. Among 32 612 kanamycin-resistant transformants, 33 strains that reproducibly formed smaller colonies than the parental strains were confirmed to have defects in A motility by microscopic examination of the edge of their colonies. Fifteen of the mutants lacked the thin and crenellated edges indicative of swarm spreading. The remaining 18 mutants retained some A motility, but it was noticeably less than the parents.

Visualizing slime secretion

Many A^+ cells depositing and following slime trails are shown in Fig. 1A and B. Figure 1C–H show several frames of a movie made by Lars Jelsbak of two well-separated gliding cells. Each leaves a slime trail, reverses several times, and with each reversal follows, extends and thickens its own trail. The trail elongates progressively at both ends of these reversing cells, clearly demonstrating a moment by moment correlation between movement and the deposition of slime. Slime has been stained with acridine orange, a non-specific fluorescent dye (Wolgemuth *et al*., 2002). In the present study, extrusions from A^+ cells were visualized without staining by means of differential interference contrast (DIC) microscopy. The refractive index difference between slime and the glass of a microscope slide renders the slime visible, and is consistent with a polysaccharide gel. Figure 2 shows representative cells, each of them have a single ribbon of slime in line with the axis of the cell, and only at one end of each cell. None of the more than 200 wild-type (A^+S^+) cells examined critically had ribbons at both ends, in agreement with the observations on

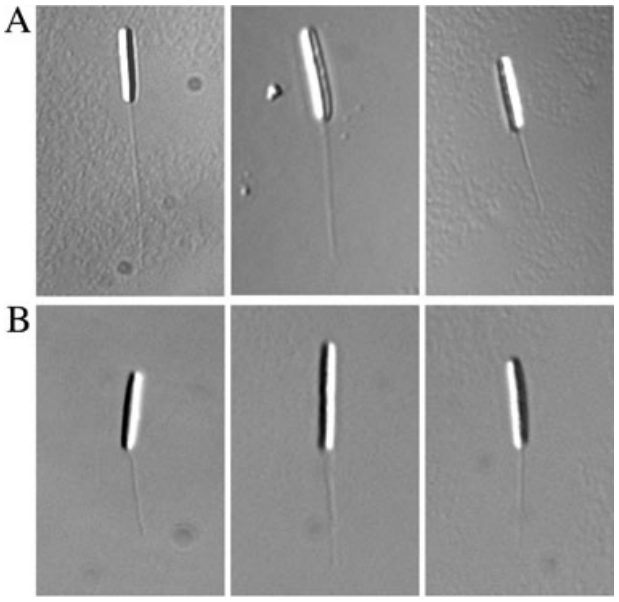

Fig. 2. Visualization of slime extruded from individual wild-type *M. xanthus* cells. Panel A, A^+S^+ DK1622; panel B, A^+S^- DK10410. Cells that had been deposited on the bottom of a plastic tissue culture plate were incubated overnight. After gentle harvest, the cells were transferred to a microscope slide. They were photographed at 100× under oil immersion using a DIC objective.

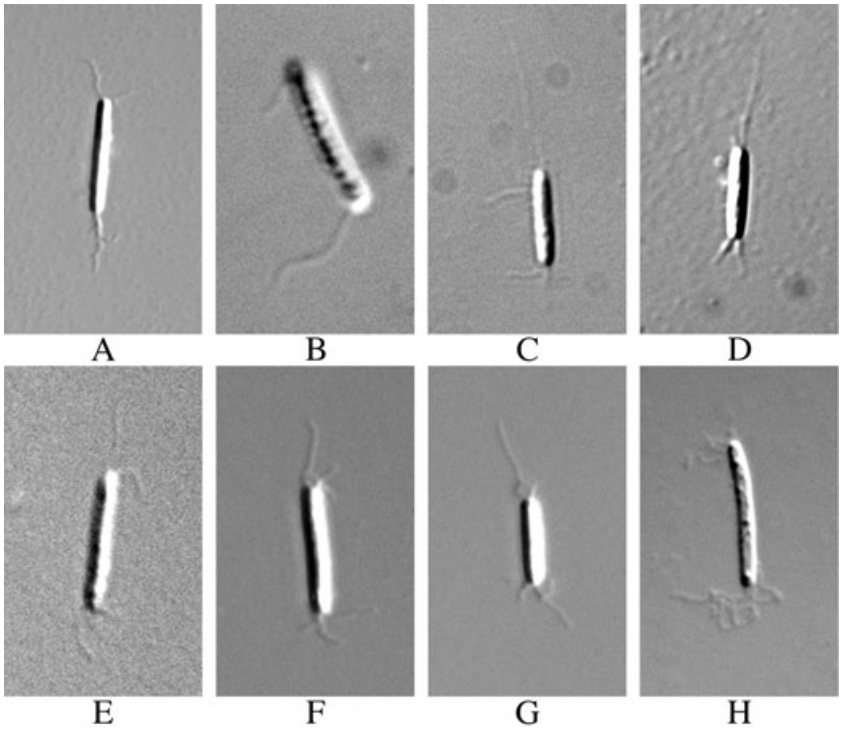

Fig. 3. Slime distributions in the non-motile (A^-S^-) mutants. Cells were prepared and examined as described in the legend to Fig. 2.
A. *agmK*::TF (DK13001).
B. *agnA*::TF (DK13002).
C. *mglA*::TF (DK13003).
D. *agmX*::TF (DK13004).
E. *agnB*::TF (DK13005).
F. *agnC*::TF (DK13006).
G. *aglU*:TF (DK13007).
H. *cglB*::TF (DK13008).

acridine-stained cells (Wolgemuth *et al*., 2002). At any instant, slime secretion from normal cells was always polar and restricted to one end of each cell.

By contrast, the seven non-motile mutants isolated from DK10410 and one from DK8615 extruded slime from both poles (Fig. 3). These strands of slime were thinner, more curved than the A^+ slime, and the slime filaments tended to angle away from the long axis of the cell. We suggest that bipolar extrusion causes the loss of A motility. Finally, the mutants with partial A motility showed unipolar extru-

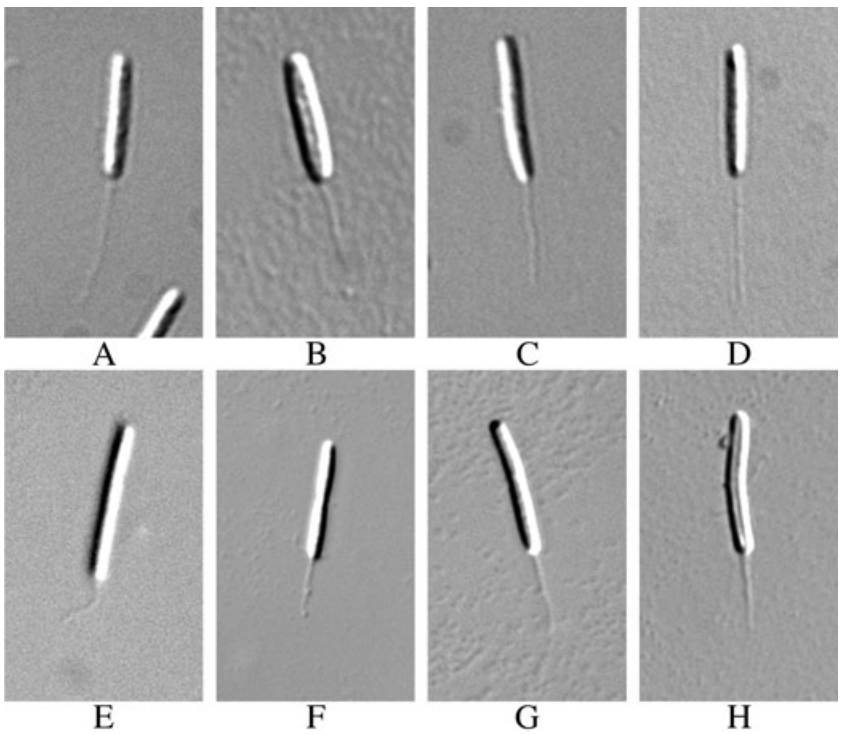

Fig. 4. Slime distributions in the partial A motile mutants. Cells were prepared and examined as described in the legend to Fig. 2.
A. *pglB*::TF (DK13010).
B. *pglC*::TF (DK13011).
C. *pglE*::TF (DK13013).
D. *pglF*::TF (DK13014).
E. *pglH*::TF (DK13016).
F. *pglJ*::TF (DK13018).
G. *mglB*::TF (DK13020).
H. *pglK*::TF (DK13021).

sion (Fig. 4). We refer to these mutants as *pgl*, to indicate their partial gliding motility.

Quantifying partial A motility

To investigate why the *pgl* mutants form smaller colonies, their rates of swarm expansion were measured. Swarm expansion rates summarize the net outward movement of thousands of cells, mostly in a single layer, which constitutes the edge of a colony of motile cells. Figure 5 shows that swarms of 14 *pgl* mutants expanded at rates from just slightly greater than DK11316 (A^-S^-) to almost as large as DK10410 (A^+S^-). (Four of the 18 total mutants were unavailable for testing at the time of this experiment.) DK10410, one of the parental A^+S^-strains, possesses full A motility. DK11316, an A^-S^- strain that carries null mutations in *cglB* and in *pilA* is non-motile and a negative control. It had the slowest rate, which measures colony expansion solely due to growth and cell division. All strains had similar growth rates measured in liquid culture (data not shown). Each *pgl* swarm expanded at a roughly constant rate (Fig. 5A and B), but each rate was lower than the A^+ and higher than the A^- controls, and the rates spread continuously across the available range.

To test the possibility that partial A motility might arise from a polar effect of the transposon insertion on a downstream motility gene, an in-frame deletion mutant was constructed for comparison. The *pglJ* gene, which is adjacent to genes that might be co-transcribed with it, was deleted and the rate of swarm expansion was measured. The Δ*pglJ* strain had a swarm rate that is 63% of a fully A-motile strain (DK10410), compared with the 76% of the *pglJ*::TF (the pMiniHimar-*lacZ* insertion mutant) (Fig. 5C). These data show that this mutant's partial motility is not caused by polarity on a downstream gene but is more likely the direct consequence of the total inactivation of *pglJ*. The possibility that the transposon had inserted into the C-terminal region of each of the *pgl* genes leaving some residual function was examined through sequencing the myxobacterial DNA adjacent to the transposon in each mutant. It is indicated in the sequence section below that each of the insertions would have been expected to inactivate their target gene.

Cells at the leading edge of a swarm have different orientations which direct their movement, and that movement is sporadic: cells move, stop and start again (Jelsbak and Søgaard-Andersen, 1999). Frequently after stopping, a cell reverses its gliding direction (Kuhlwein and Reichenbach, 1968; Blackhart and Zusman, 1985). To see how *pgl* function contributes to swarm expansion, time-lapse movies were made of pgl^+ and pgl^- strains at low cell density in order that individual cells could be tracked. Three parameters of movement were measured on individual cells: the fraction of cells in a given microscopic field that moved in 15 min, termed the movement probability; the reversal frequency; and the cell speed when they were moving. Comparing A^+ with *pgl* discriminated between several possible explanations for a reduction in swarm rate. First, *pgl* cells might pause for a longer time between moves than A^+ cells. Indeed, all five *pgl* mutants examined had half or less the probability of movement than the A^+ strain, indicating longer pause times (Table 1).

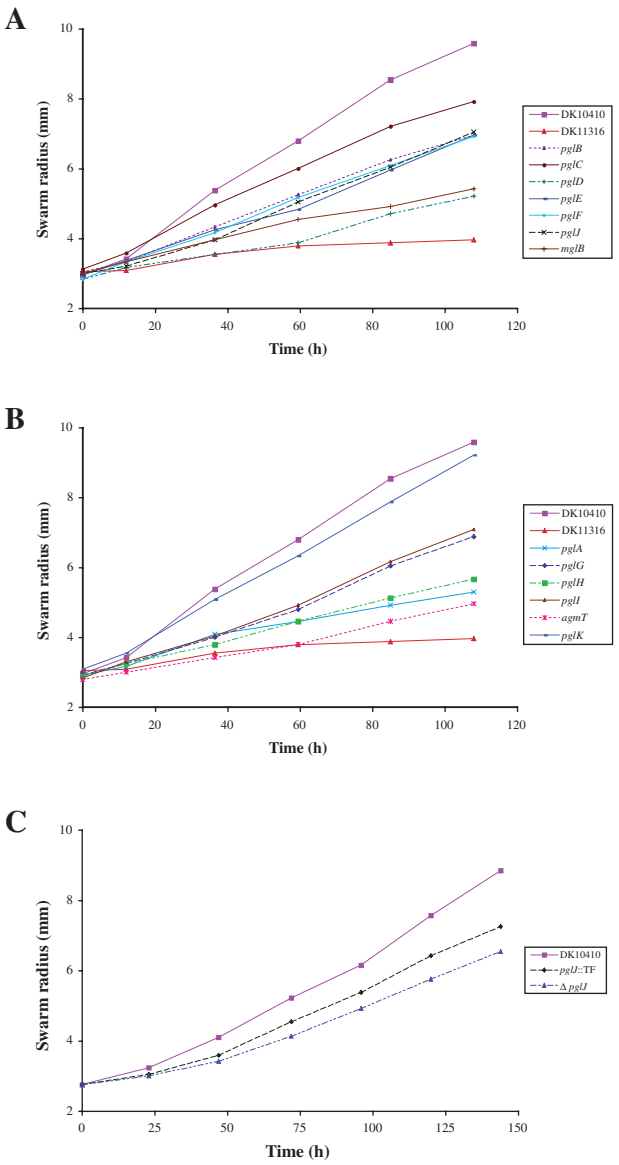

Fig. 5. Expansion of A^+S^- and *pgl* mutant swarms. The radius of the swarm on CTT agar plates incubated at 32°C is shown as a function of time.
A and B. Expansion rates of the partial A motile *M. xanthus* strains are compared with the A^+S^- strain DK10410 and the non-motile A^-S^- strain DK11316. Only the partial A motile mutants generated in DK10410 background were used in this experiment.
C. Swarm expansion rates of the in-frame deletion mutant Δ*pglJ* (DK13024) and the transposon-inserted mutant *pglJ*::TF (DK13018) are compared with DK10410 as a control.

Table 1. Movement probability, reversal frequency and gliding speed.

Strain	Movement probability ± SD (*n*)	Reversal frequency (reversals h^{-1} ± SD)	Gliding speed (μm min^{-1} ± SD)
DK10410 (A^+)	0.63 ± 0.007 (563)	6.00 ± 2.41	1.42 ± 0.32
DK13010 (*pglB*::TF)	0.34 ± 0.01 (406)	5.27 ± 2.81	1.13 ± 0.23
DK13013 (*pglE*::TF)	0.18 ± 0.01 (559)	6.01 ± 3.28	1.24 ± 0.26
DK13014 (*pglF*::TF)	0.21 ± 0.01 (431)	4.24 ± 2.82	N/A
DK13016 (*pglH*::TF)	0.18 ± 0.01 (386)	12.13 ± 3.74	N/A
DK13020 (*mglB*::TF)	0.36 ± 0.01 (525)	5.31 ± 2.50	N/A

Second, a lower swarm expansion rate might result from a change in the number of reversals per unit time (reversal frequency). Cells with a very high reversal frequency would be expected to have a lower swarm rate because they would spend more time reversing than moving. Reversal frequencies were measured on isolated cells of A^+ and five *pgl* mutants in the time-lapse movies. The mutants were found to have the same reversal frequency, within experimental error, as the A^+ in Table 1, except for *pglH*, which had twice the reversal frequency of A^+. A third possibility is that each cell might move more slowly when it does move, but no significant speed differences were detected (Table 1). The average speed of A^+ (DK10410) cells might be slightly greater than either the *pglB* or *pglE* mutant, which could be an indirect consequence of their lower movement probabilities.

Finally, the possibility of a *pgl* effect on cell flexibility or cell–cell cohesion that would indirectly affect movement was considered. Gliding cells bend and change their gliding direction when they strike another cell or other impediment on the agar surface. If *pgl* mutants bent more easily or cohered differently to each other than the A^+, a qualitatively different distribution of cells at the edge of the swarm might be expected. To explore these and related possibilities, the time-lapse movies of the edge of swarm zones of a partially motile mutant were compared with those of A^+S^- and A^-S^- strains. The swarm zone of DK10410 cells, the parental strain with full A motility, is shown in Fig. 6A. A^-S^- mutant cells did not move beyond the sharp edge of the colony at any time during the 60 min recording (Fig. 6D). Expansion of a non-swarming A^-S^- colony is due to cell growth and cell division, motility is not involved; consequently the A^-S^- strain expands at the lowest rate in Fig. 5. If there is no change in the distribution of *pgl* mutant cells, as the swarm expansion rate of the *pglJ* mutant is 60% that of the A^+ strain, one might expect that the cell and slime trail distribution of *pglJ* at 90 min would resemble the A^+ at 54 min (60% of 90 min). Figure 6B shows the 54 min frame from the 90 min movie of the A^+S^-, and indeed, the 90 min frame of the *pglJ* mutant (Fig. 6C) shows a pattern of slime trails, trail curvatures, trail length and cell distributions that qualitatively resemble Fig. 6A and B. In sum, the major effect of the loss of *pgl* function appears to be a lower probability of movement, resulting from longer pauses.

Elasticotaxis

Partial motility is also manifest in elasticotaxis. Elasticotaxis, first described by Stanier in 1942, measures the preference of myxobacterial cells to glide along lines of stress in an agar gel on which they are moving (Stanier, 1942). Elasticotaxis can be measured by the ratio of the rate of swarm spreading in the direction of stress in the agar to the rate perpendicular to the stress (Fontes and Kaiser, 1999). On unstressed agar, the rate of spreading

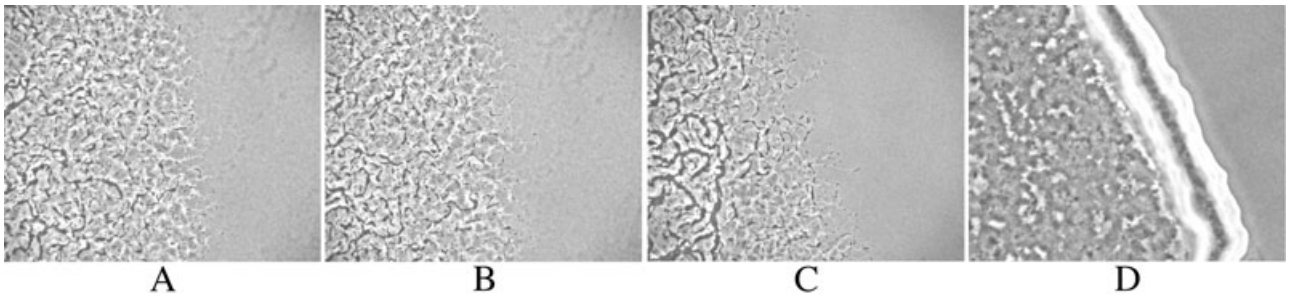

Fig. 6. Distribution of *M. xanthus* cells in the spreading zone. Individual frames from the time-lapse movies whose preparation is described in *Experimental procedures* for photomicroscopy.
A. DK10410 (A^+S^-) at 90 min.
B. DK10410 (A^+S^-) at 54 min.
C. Partially A motile *pglJ*::TF (DK13018) at 90 min.
D. DK11316 (A^-S^-) at 60 min.

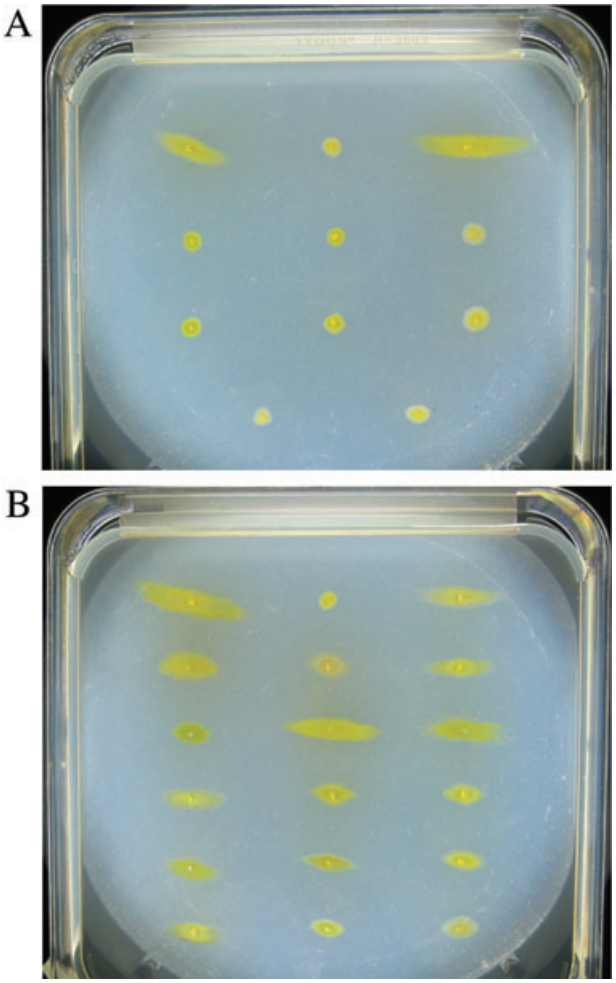

Fig. 7. Elasticotaxis of *M. xanthus* mutant strains. Square plates with plastic tubes inserted at the top to generate stress were inoculated by toothpick on a grid.
A. *M. xanthus* control strains and non-motile mutants. Grid location 1,1: A^+S^- (DK8615); 1,2: A^-S^- (DK11316); 1,3: A^+S^- (DK10410); 2,1: *agmK*::TF (DK13001); 2,2: *agnA*::TF (DK13002); 2,3: *mglA*::TF (DK13003); 3,1: *agmX*::TF (DK13004); 3,2: *agnB*::TF (DK13005); 3,3: *agnC*::TF (DK13006); 4,1: *aglU*::TF (DK13007); 4,2: *cglB*::TF (DK13008).
B. *M. xanthus* control strains and partial A motile mutants. Grid location 1,1: A^+S^- (DK10410); 1,2: A^-S^- (DK11316); 1,3: A^+S^- (DK8615); 2,1: *pglA*::TF (DK13009); 2,2: *pglB*::TF (DK13010); 2,3: *pglC*::TF (DK13011); 3,1: *pglD*::TF (DK13012); 3,2: *pglE*::TF (DK13013); 3,3: *pglF*::TF (DK13014); 4,1: *pglG*::TF (DK13015); 4,2: *pglH*::TF (DK13016); 4,3: *pglI*::TF (DK13017); 5,1: *pglJ*::TF (DK13018); 5,2: *agmT*::TF (DK13019); 5,3: *mglB*::TF (DK13020); 6,1: *pglK*::TF (DK13021); 6,2: *pglM*::TF (DK13022); 6,3: *pglN*::TF (DK13023).

is the same in all radial directions and the swarm is circular, while on stressed agar the swarm is elliptical. The major axis of the resulting ellipse coincides with the direction of the stress. The elasticotactic responses of all the A motility mutants isolated in the DK10410 background and described above were measured as shown in Fig. 7. The eight non-swarming (A^-S^-) mutants tested showed no elasticotaxis; their colonies were circular on stressed agar (Fig. 7A). Evidently, the direction of cell growth shows little or no response to substrate stress. Elasticotaxis was evident in all 15 mutants that have partial A motility (Fig. 7B). Their swarms were elliptical, and in every case the major axis of the ellipse was coincident with the direction of stress (Fig. 7B). The elasticotaxis coefficients of the *pgl* mutants were less than an A^+S^- strain but greater than an A^-S^- strain. Strikingly, the elasticotaxis coefficients of the partially motile mutant strains are directly proportional to their swarm rates. The numerical correspondence shown in Fig. 8 strongly suggests the swarm expansion rates and the elasticotaxis coefficients are different expressions of a common cause. Despite a superficial similarity between the assays for elasticotaxis and swarm expansion, their proportionality is not trivial; swarm expansion averages the outward movement of many cells and has the dimensions of a velocity; the elasticotaxis coefficient measures the asymmetry of movement direction and is dimensionless. Thus the two measures of motility are fundamentally different; their correlation is not trivial.

Functions of genes whose destruction gives partial motility

With data from the TIGR/Monsanto sequence of *M. xanthus* (GenBank CP000113), the coding sequences (CDS) disrupted by *Himar* were identified by cloning and sequencing a short segment adjacent to the transposon insertion in each mutant. All disrupted CDS could be rec-

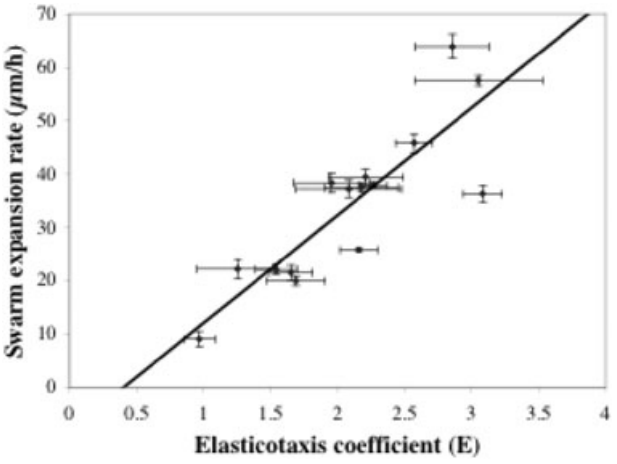

Fig. 8. The swarm expansion rate plotted against the elasticotaxis coefficient (E) for the partial A motile mutants. Rates of swarm expansion were taken from Fig. 5. *E*-values were obtained from Fig. 7 as the ratio of the diameter parallel to the compressing plastic tube and perpendicular to it. Error bars indicate one SD on either side of the mean measured value of E. The least-squares linear regression line is drawn on the figure, and the mean r^2 for experimental points about that line is 0.736.

ognized unambiguously in the published sequence. The complete CDS of each (uninterrupted) gene was then compared with the public protein databases, using Protein–Protein BLAST, to identify the most likely biochemical function of each A motility gene product by sequence similarity to known proteins. The highest-scoring hits to proteins that have catalytic functions corresponding to all the mutants isolated in this study are listed in Table 2. Some genes were hit more than once: *agmK* was hit six times (putatively it is a large gene, encoding 3822 amino acids), *agmX*, *cglB*, *pglA*, *pglF* and *mglB* were each hit twice. Deletion of *mglB* had previously been shown to markedly decrease the stability of MglA protein (Stephens and Kaiser, 1987; Stephens *et al*., 1989; Hartzell and Kaiser, 1991). Because swarming depends on MglA (Hodgkin and Kaiser, 1979a,b; Kaiser, 2007), *mglB* was, in fact, the first gene knockout mutant established to exhibit partial A motility. Isolation of new *mglB* mutants demonstrates the sensitivity of the mutant screen that was employed for reductions in A motility. The other genes listed in Table 2 will be examined below in light of their putative functions.

Discussion

New evidence is presented here that links A motility with the biosynthesis of, and gel formation by, a polysaccharide in *M. xanthus*. The new evidence complements high resolution electron micrographs which revealed several hundred thick walled rings, 80% of which were located at the cell poles (Wolgemuth *et al*., 2002). The rings are thought to be end views of secretory nozzles. Near the rings, narrow ribbons of an amorphous material, interpreted as a polysaccharide gel, were observed in the course of extrusion from cell ends (Wolgemuth *et al*., 2002). Evidently several narrow ribbons fuse laterally to form the single unipolar ribbon seen by light microscopy (Fig. 2). In an aqueous environment, ribbons of a polysaccharide gel would be expected to fuse. Both electron and light microscopy showed that the gel ribbons were to be found only at one cell pole at any particular moment; they were always absent from the opposite pole of the cell. Unipolarity of the extruded ribbons parallels unidirectional cell movement. As a consequence of gel extrusion, A^+S^+ cells leave a phase bright trail of slime when they move (Reichenbach *et al*., 1965; Burchard, 1982; Wolgemuth *et al*., 2002 and Fig. 1). Slime extrusion at the back ends of many cells is shown in that figure. Fig. 1A and B show that every cell is on a slime trail. Figure 1C–H show how the trail grows as slime is deposited. It has been calculated that the swelling of a polysaccharide (slime) gel as it hydrates could produce a force sufficient for cells to glide at the speed observed (Wolgemuth *et al*., 2002; Wolgemuth, 2005).

The major new finding of this study is that all the new mutant strains identified because they had lost some or all of their A motility prove to have defects in their secretion of slime. Almost half (15/33) of the new mutants have completely lost A motility. They are non-motile because they are secreting slime and therefore push from both of their ends simultaneously. Because the force is comparable at both ends, they are unable to make progress in either direction. The majority (18/33) of the A motility mutants secrete slime only from one end of the cell. However, they are only partially A motile, they have a lower rate of swarm expansion and a proportionately lower coefficient of elasticotaxis than *pgl*$^+$. They have defects in slime secretion that lowers their movement probability. The two sets of mutants show a perfect correlation between A motility and *unipolar* slime secretion. These data in themselves are a strong argument that slime secretion drives A motility. But, having visualized slime and seen its effects on cell movement, we need to understand its chemistry to see how force might be developed. The *pgl* mutants connect us to the enzymology of A motility: six *pgl* mutants carry null mutations in genes annotated as glycosyltransferases or other enzymes of polysaccharide biosynthesis.

Like *pglB*, almost all the partially motile mutants have wild-type reversal frequency, wild-type gliding speed, but a decreased movement probability compared with wild type (Table 1). According to Table 2, PglB protein is expected to have glycosyltransferase activity because it strongly resembles a glycosyltransferase of *Leptospira interrogans* (the value of the expectation, $E = 3e\text{-}81$). Enzymes of this type are needed to transfer an activated sugar (a UDP, ADP, GDP or GMP linked sugar) to a variety of substrates (Campbell *et al*., 1997). PglB, a glycosyltransferase of group 1, is a member of pfam00534. The second Pgl protein in Table 2, PglF is predicted to have two different glycosyltransferase domains: one in the N-terminal half that resembles RfaG, COG0438 and the glycosyltransferases of group 1. These enzymes are expected to transfer an activated sugar to an oligosaccharide acceptor. The more C-terminal glycosyltransferase domain of PglF belongs to group 2 that transfer sugar from UDP-glucose, UDP-N-acetyl-galactosamine, GDP-mannose or CDP-abequose to a range of acceptors like dolichol phosphate, teichoic acid and cellulose (Table 2). Growing polysaccharide chains in bacteria are generally anchored to a membrane by undecaprenylphosphate (Raetz and Whitfield, 2002), and the group 2 transferase of PglF may catalyse formation of Und-PP-oligosaccharides. The third Pgl protein in Table 2, PglD, has a nucleotidyl transferase domain (PF00483) and a mannose-1-phosphate isomerase domain (PF01050). This suggests that it may catalyse the synthesis of GDP-mannose for the synthesis of a mannose containing polysaccharide. PglN encodes a bifunctional ADP

Table 2. Inferred function of disrupted A motility genes.

Coding sequence[a]	Gene	Knockout phenotype	Domain function	Sequence *E*-value[b]	Conserved domains[c]
MXAN2921	*pglB*	Partially A motile	Glycosyltransferase similar to YP 000604 of *Leptospira interrogans*	3.00E-81	Pfam00534
MXAN4616	*pglF*	Partially A motile	Glycosyltransferase 1 domain and glycosyltransferase 2 domain	CDD 40621, 1e-18 CDD 40622, 6e-18	COG0438
MXAN6501	*pglD*	Partially A motile	GDP-mannose synthesis		PF00483 PF01050
MXAN4710	*pglN*	Partially A motile	ADP-heptose synthase, bifunctional sugar kinase/adenylyltransferase RfaE_like	cd01172, 9e-51	COG2870
MXAN2919	*pglJ*	Partially A motile	Integral membrane protein similar to *S. coelicolor* gi:1098142 with local similarity to Wzy_C polymerase	IPR007016, 6.00E-07	PF04932
MXAN7252	*pglA*	Partially A motile	Exopolysaccharide synthesis, ExoD		PF06055
MXAN4148	*pglK*	Partially A motile	Predicted transmembrane transcriptional regulator	3.00E-12	COG5662
MXAN5319	*pglC*	Partially A motile	TPR repeat	*Anaeromyxobacter dehalogenans*[b] 5.00E-60	NCBI cdd00189
MXAN4867	*pglI*	Partially A motile	Hypothetical abductin-like protein (*M. xanthus*[b])		None
MXAN5382	*aspT*	Partially A motile	tRNA-Asp		
MXAN5585	*pglE*	Partially A motile	Glycosyltransferase of PMT family	gi13582, 6e-14	COG1807
MXAN6607	*agmT*	Partially A motile	Predicted periplasmic solute-binding protein (*Trichodesmium erythraeum*)		COG1559
MXAN7160	*pglM*	Partially A motile	Alanine racemase		COG0787
MXAN1926	*mglB*	Partially A motile	guanine nucleotide exchange factor for MglA		NOG46155
MXAN2050	*pglH*	Partially A motile	TPR repeat, CheY-like receiver domain, and a winged-helix DNA-binding domain		COG0745
MXAN1925	*mglA*	Non-motile (A^-S^-)	SAR1-like small GTPase		COG1100
MXAN2541	*agnA*	Non-motile (A^-S^-)	Unknown		None
MXAN3008	*aglU*	Non-motile (A^-S^-)	WD-repeat lipoprotein, acylaminoacyl-peptidase		COG1506
MXAN3060	*cglB*	Non-motile (A^-S^-)	Outer membrane lipoprotein		cd01456
MXAN4862	*agmX*	Non-motile (A^-S^-)	Outer membrane lipoprotein		COG2885
MXAN4863	*agmK*	Non-motile (A^-S^-)	TPR repeat protein		COG0457
MXAN6403	*agnB*	Non-motile (A^-S^-)	ABC-type transporter permease protein (*Vibrio fischeri*)		COG4591
MXAN7296	*agnC*	Non-motile (A^-S^-)	Unknown		None

a. Gene number in the complete *M. xanthus* genome, GenBank CP000113.
b. ID of the best match in the NCBI protein database, *E*-value is expected matching by chance.
c. COG, Clusters of Orthologous Groups of proteins, NCBI; NOG, non-supervised orthologous group, STRING database (http://string.embl.de/).

heptose synthetase, RfaE (Table 2), which suggests that a heptose could be one of the sugars in the slime polymer. PglJ is similar to an integral membrane glycosyltransferase, PF04932 (Table 2). Because PglA has four predicted transmembrane domains, it is likely to be a transmembrane protein that aligns over 200 residues with ExoD (Table 2). ExoD is involved in exopolysaccharide production in *Sinorhizobium meliloti* and is required for nodule invasion (Reed and Walker, 1991; Cheng and Walker, 1998).

The *S. meliloti* ExoD product is a repeating heteropolymer – a repeat unit polysaccharide, or RUP for short. Due to their medical importance, most enzymatic studies of RUP biosynthesis have been carried out on the O-antigen-specific chains of lipopolysaccharide (Raetz and Whitfield, 2002) and the capsules of *Escherichia coli* (Whitfield and Roberts, 1999). In both lipopolysaccharide and capsules, biosynthesis of a repeat unit of the polysaccharide begins on the cytoplasmic face of the inner membrane and continues during translocation to the periplasmic face of the inner membrane where repeat units are joined together before secretion (Raetz and Whitfield, 2002). Typically each biosynthetic step requires a distinct membrane-localized glycosyltransferase that hands its products off to another one, as reviewed by Raetz and Whitfield (2002). A handing off action is clearly implied by the structure of PglF, which has two different glycosyltransferase domains. Thus, the findings that *pglB*, *pglF*, *pglD*, *pglN* and *pglA* encode glycosyltransferases, and that *pglJ* is the functional homologue of one of the three integral membrane polymerases for RUP synthesis (Table 2) strongly suggest that the *pgl* enzymes catalyse the biosynthesis of an RUP whose unipolar secretion propels the cell.

PglC contains five tetratrico peptide repeats (TPRs, NCBI cd00189, Table 2). A homologue has been found in *Anaeromyxobacter dehalogenans* with an *E*-value of 5e-60. TPR structural motifs are present in a wide range of proteins that assemble membrane-localized multiprotein complexes (D'Andrea and Regan, 2003). Just as TgI with six TPR motifs is an assembly factor for the PilQ secretin in the outer membrane of *M. xanthus* (Nudleman *et al*., 2006), PglC could be an assembly factor for a putative RUP biosynthetic complex of Pgl proteins in the inner membrane. The entire length of PglK has weak similarity to a transmembrane anti-sigma factor, COG5662 (Table 2) and it is just downstream of the ECF sigma factor *rpoE1* (Ward *et al*., 1998). Ward *et al*. reported that knockout mutants of *pglK* (their *orf5*) were able to swarm and to aggregate in two genetic backgrounds. That diagnosis is not inconsistent with partial A motility.

The transposon insertions in the *pgl* mutants did not cluster in the carboxy end of the corresponding CDS, so they would not have been expected to leave partial enzyme activity. Is it possible that gene knockout engenders partial motility? Five *pgl* mutants tested in Table 1 pause twice as long between gliding movements as an A^+ strain. We think it likely that the PglB, PglF, PglD, PglN, PglJ and PglA knockout mutants are also pausing in their synthesis of the propulsive polysaccharide for the lack of a glycosyltransferase. And because *M. xanthus* encodes many glycosyltransferases, needed for its multiple polysaccharides, it is possible that the lack of a particular transferase in an RUP biosynthetic pathway could be mitigated by a glycosyltransferase from another RUP pathway that happens to fit into the slime synthesizing enzyme complex. However, incorporating an alternate transferase into a multiprotein assembly complex would take time, thus pausing and interrupting polymerization. Moreover, a mitigated complex is likely to be less stable than the wild-type complex; it may have to be repeatedly reformed, introducing more pauses. Pausing clearly would be expected to decrease the swarm expansion rate. Because the incorporation of a mitigating sugar might change the sequence of sugars, it would be expected to affect interactions between the resulting polymer chains. If elasticotaxis is due to gelation of slime with the polysaccharides of agar, a reduction in the elasticotaxis coefficient would be expected as well.

pglH and *mglB m*ost likely have partial A motility for reasons other than RUP synthesis. PglH mutants increase the reversal frequency (Table 1); and *pglH* encodes a response regulator with a TPR repeat that is related to PleD; it is not a glycosyltransferase (Table 2). PglH is more likely to change the reversal frequency as a component of the reversal clock (Kaiser, 2007). The mutant phenotype suggests that the reversal frequency of wild type has evolved to maximize the rate of swarm expansion, so that an increase in the reversal frequency is likely to decrease the overall swarm rate. Although the *mglB* mutant has a normal reversal frequency (Table 1), MglB is a guanine nucleotide exchange protein (Table 2) that is expected to work with the MglA GTPase, to reverse cell polarity (Kaiser and Yu, 2005). MglB would catalyse release of GDP bound to the GTPase, promoting its replacement by GTP (Bourne *et al*., 1991). It has long been known that an *mglB* mutant swarms at a low rate and has little residual A motility (Stephens and Kaiser, 1987; Hartzell and Kaiser, 1991), and its movement probability is about half that of A^+ (Table 1).

As mentioned above, approximately half the new mutants eliminated A motility; all of them secreted slime simultaneously from both ends of each cell. We suggested that these mutants are non-motile because they have lost the unipolarity of slime secretion that is essential for cell movement. The observation that bipolar mutants of *M. xanthus* are non-motile directly links a bipolar slime secretion morphology to the lack of movement. The pro-

totypic bipolar mutant is *mglA*, which was discovered by Hodgkin and Kaiser (1979a) who showed that it blocked both A motility and S motility. As mentioned, MglA is a GTPase switch that maintains the unipolarity of both the A and the S engines (Kaiser, 2007), and that ensures they have opposite polarity (Kaiser, 2003). MglA mutant cells had been observed to oscillate back and forth rapidly (Spormann and Kaiser, 1999). However, with each oscillation they move less than 1/5 of a cell length, and make no significant progress in either direction (Spormann and Kaiser, 1999). The rapid reversals of *mglA* mutants are not due to signals from the reversal generator because they lack an essential constituent of the generator. Instead, we suggest those reversals are a statistical consequence of active slime secretion from both ends. A calculation made by Charles Wolgemuth shows that the speed distribution of oscillating Δ*mglAB* cells can be deduced from the known speed distribution of Δ*mglB* cells (Spormann and Kaiser, 1999), assuming that the two ends of the same cell secrete independently (Kaiser, 2007).

All the proteins found in this study to be essential for unipolar slime secretion are listed at the bottom of Table 2. The second member of that list after MglA is CglB: the Δ*cglB* mutant also secretes slime from both ends (Fig. 3) and the cells oscillate 10-fold faster than A^+, like Δ*mglA* (Spormann and Kaiser, 1999), which indicates a failure of the normal polarity switching mechanism. However, *cglB* mutants only affect A motility; their S motility is normal (Hodgkin and Kaiser, 1979a). Whereas MglA is cytoplasmic, CglB is a lipoprotein with a type II signal sequence (Rodriguez and Spormann, 1999) that resides in the outer membrane (Simunovic *et al*., 2003). In addition, CglB is transferred with high efficiency by stimulatory contact between cell ends (Hodgkin and Kaiser, 1977; White and Hartzell, 2000; Nudleman *et al*., 2005); this confirms its identification as a motility-related, outer membrane lipoprotein. Other non-motile mutants isolated in this study were also shown to have slime emerging from both poles by DIC microscopy (Fig. 3). Several had been identified as critical for A motility (White and Hartzell, 2000; Youderian *et al*., 2003). AgnA, AgnB and AgnC proteins are new. AgnB is homologous to a permease component of an ABC transporter from *Vibrio fischeri* which may be involved in localizing a lipoprotein (Table 2). Another bipolar mutant, AgnC, has a stretch of hydrophobic amino acids in its conceptually translated sequence suggesting that it is a transmembrane protein. Several old (AglU, AgmK, AgmX), and new (AgnB, AgnC) are either membrane proteins, or proteins involved in lipoprotein release. Their unknown roles could be related to that of CglB.

If *M. xanthus* is propelled by slime secretion, as proposed, then it is remarkable that none of the searches for A motility mutants have turned up mutants lacking slime. Despite extensive mutant hunts and frequent microscopic searches for locomotor organelles (Burchard *et al*., 1977; Pate and Chang, 1979; Burchard, 1981; 1984; Lunsdorf and Schairer, 2001), no alternative motility mechanism has survived initial experimental testing. There is, however, an alternative speculation based on Lapidus and Berg's observation of energy-dependent movements of small particles adhering to *Cytophaga* U67 cells (Lapidus and Berg, 1982). After observing similar particle movement on the surface of *Flexibacter johnsoniae*, Dr M.J. McBride developed a mechanically complete model for gliding (McBride, 2000). The model proposes that mobile cell surface proteins in the *F. johnsoniae* outer membrane bind the substratum. Other proteins in the cytoplasmic membrane are proposed to harvest the proton motive force to propel yet other proteins that are embedded in the outer membrane along tracks that are attached to the peptidoglycan. Finally, processive attachment and detachment of the outer membrane proteins to the substratum are proposed to produce a walking motion. Might such a machine explain A motility? McBride's mechanism predicts motorized binding proteins, perhaps AAA ATPases (Vale, 2000). On the one hand, none of the Mgl, Agm or Agn proteins have ATPase function, but a failure to find predicted proteins cannot be deemed a disproof. On the other hand, finding multiple glycosyltransferases, finding a strong preference to follow slime trails and finding sensitive elasticotactic orientation seem difficult to reconcile with the McBride mechanism of gliding. In our view, it makes more sense to hypothesize that slime secretion is vital, for reasons to be found. Perhaps the accumulation of intermediates in slime production is toxic to cells, or perhaps slime production facilitates survival after electroporation.

Experimental procedures

Bacterial strains

Strains and plasmids employed are listed in Table 3. In addition *E. coli* strains DH5α lpir and TOP10 were used as hosts for cloning. They were grown in Luria–Bertani broth (LB) or on 1.5% agar LB plates supplemented with kanamycin (50 μg ml^{-1}) or ampicillin (100 μg ml^{-1}) as needed. *M. xanthus* DK1622 and its S motility mutant strains DK10410 and DK8615 were routinely grown in CTT medium [1% Casitone, 10 mM Tris-HCl (pH 8.0), 8 mM $MgSO_4$, 10 mM KPO_4 (pH 7.6)] at 32°C or on 1.5% agar CTT plates containing 40 μg ml^{-1} of kanamycin or 12.5 μg ml^{-1} of oxytetracycline when required. Plasmid pMiniHimar-*lacZ* was the donor of the mini-*mariner* element *Himar1*. pMiniHimar-*lacZ* DNA was prepared using the BIO-RAD Plasmid Miniprep Kit.

Transposon mutagenesis

M. xanthus DK10410 and DK8615 cells were grown to a density of 5×10^8 cells ml^{-1} in CTT broth. A 1.8 ml aliquot of the

Table 3. *M. xanthus* strains and plasmids employed.

M. xanthus strain	Genotype[a]	Phenotype[b]	Reference/construction
DK1622	Wild type	A^+S^+	Kaiser (1979)
DK8615	Δ*pilQ*	A^+S^-	Wall *et al.* (1999)
DK10410	Δ*pilA*	A^+S^-	Wu and Kaiser (1997)
DK11316	Δ*cglB pilA*::tet^R	A^-S^-	Fontes and Kaiser (1999)
DK13001	*agmK*::TF	A^-S^-	pMiniHimar-l*acZ* × DK10410, select Kan^R, screen for A^-
DK13002	*agnA*::TF	A^-S^-	pMiniHimar-l*acZ* × DK10410, select Kan^R, screen for A^-
DK13003	*mglA*::TF	A^-S^-	pMiniHimar-l*acZ* × DK10410, select Kan^R, screen for A^-
DK13004	*agmX*::TF	A^-S^-	pMiniHimar-l*acZ* × DK10410, select Kan^R, screen for A^-
DK13005	*agnB*::TF	A^-S^-	pMiniHimar-l*acZ* × DK10410, select Kan^R, screen for A^-
DK13006	*agnC*::TF	A^-S^-	pMiniHimar-l*acZ* × DK10410, select Kan^R, screen for A^-
DK13007	*aglU*::TF	A^-S^-	pMiniHimar-l*acZ* × DK10410, select Kan^R, screen for A^-
DK13008	*cglB*::TF	A^-S^-	pMiniHimar-l*acZ* × DK8615, select Kan^R, screen for A^-
DK13009	*pglA*::TF	$A^{partial}S^-$	pMiniHimar-l*acZ* × DK10410, select Kan^R, screen for A^-
DK13010	*pglB*::TF	$A^{partial}S^-$	pMiniHimar-l*acZ* × DK10410, select Kan^R, screen for A^-
DK13011	*pglC*::TF	$A^{partial}S^-$	pMiniHimar-l*acZ* × DK10410, select Kan^R, screen for A^-
DK13012	*pglD*::TF	$A^{partial}S^-$	pMiniHimar-l*acZ* × DK10410, select Kan^R, screen for A^-
DK13013	*pglE*::TF	$A^{partial}S^-$	pMiniHimar-l*acZ* × DK10410, select Kan^R, screen for A^-
DK13014	*pglF*::TF	$A^{partial}S^-$	pMiniHimar-l*acZ* × DK10410, select Kan^R, screen for A^-
DK13015	*aspT*::TF	$A^{partial}S^-$	pMiniHimar-l*acZ* × DK10410, select Kan^R, screen for A^-
DK13016	*pglH*::TF	$A^{partial}S^-$	pMiniHimar-l*acZ* × DK10410, select Kan^R, screen for A^-
DK13017	*pglI*::TF	$A^{partial}S^-$	pMiniHimar-l*acZ* × DK10410, select Kan^R, screen for A^-
DK13018	*pglJ*::TF	$A^{partial}S^-$	pMiniHimar-l*acZ* × DK10410, select Kan^R, screen for A^-
DK13019	*agmT*::TF	$A^{partial}S^-$	pMiniHimar-l*acZ* × DK10410, select Kan^R, screen for A^-
DK13020	*mglB*::TF	$A^{partial}S^-$	pMiniHimar-l*acZ* × DK10410, select Kan^R, screen for A^-
DK13021	*pglK*::TF	$A^{partial}S^-$	pMiniHimar-l*acZ* × DK10410, select Kan^R, screen for A^-
DK13022	*pglM*::TF	$A^{partial}S^-$	pMiniHimar-l*acZ* × DK8615, select Kan^R, screen for A^-
DK13023	*pglN*::TF	$A^{partial}S^-$	pMiniHimar-l*acZ* × DK8615, select Kan^R, screen for A^-
DK13024	Δ*pglJ*	$A^{partial}S^-$	pRY101 × DK10410, select Kan^R; select Gal^{R}Kan^S; screen by PCR analysis
Plasmid			
pMiniHimar-*lacZ*	Encodes the *Himar1* transposase, *aph* (kan^R), promoterless *lacZ* and oriR6K λ	Kan^R	Duan and Kaplan, University of Texas Medical School at Houston.
pBJ113	pUC118 containing kan^R and *galK*, used for constructing gene replacements	Kan^{R}Gal^S	Julien *et al.* (2000)
pRY101	Δ*pglJ*, kan^R and *galK*	Kan^{R}Gal^S	PCR-generated Δ*pglJ* fragments cloned into pBJ113

a. TF represents the transposed fragment from pMiniHimar-*lacZ* in the *M. xanthus* genes.
b. A^+, full A motility; A^-, no A motility; $A^{partial}$, partial A motility as described in *Results*; S^+, full S motility; S^-, no S motility.

culture was harvested by centrifugation, washed once with 1.8 ml of sterile water, then washed twice with 1 ml of sterile water, and resuspended in 40 μl of sterile water. Freshly washed cells were mixed with dialysed pMiniHimar-*lacZ* DNA and subjected to electroporation conditions of 0.65 kV, 400 Ω and 25 μFD in a 0.1 cm gap cuvette. The electroporated cells were immediately added to 2.5 ml of CTT broth and incubated with shaking at room temperature for 12–16 h for recovery. Recovered cells were then mixed with CTT soft agar (0.7% agar) and plated on CTT plates (1.5% agar) supplemented with kanamycin. After 5–6 days of incubation at 32°C, individual colonies were picked and transferred with sterile toothpicks on to fresh CTT agar plates. After 2–3 days of incubation at 32°C, plates were screened visually to identify small colonies and colonies with smooth edges.

Cloning of M. xanthus *genomic DNA flanking pMiniHimar*-lacZ *insertions*

Strains containing pMiniHimar-*lacZ*, described in Table 3, were grown overnight at 32°C in 10 ml of CTT broth. Bacteria were harvested by centrifugation and resuspended in 3 ml of sucrose-Tris-EDTA [25% sucrose, 10 mM Tris (pH 8.0), 1 mM EDTA (pH 8.0)]. Cells were lysed by the addition of 0.6 ml of Lytic Mix [5% sodium dodecyl sulphate, 125 mM EDTA (pH 8.0), 0.5 M Tris (pH 9.4)], and incubated at 65°C for 60 min. Proteinase K was added to 100 μg ml^{-1} final concentration and the mixture was incubated at 37°C for 2 h. *Myxococcus* genomic DNA was prepared using standard phenol-chloroform extraction and ethanol precipitation. The precipitate was suspended in 60 μl of TE [10 mM Tris-HCl (pH 8.0), 0.1 mM EDTA (pH 8.0)] overnight at 4°C and stored at –20°C. One to two microlitres of the DNA suspension was digested with 2 μl SacII restriction endonuclease for 3–12 h in a total volume of 30 μl, followed by the addition of an additional 1 μl SacII and incubation for 2 h more, and finally heated to 65°C for 15 min to inactivate the endonuclease. The digested genomic DNA was purified by phenol-chloroform extraction, ethanol precipitation, and was resuspended in 20 μl of sterile water. Digested DNA was ligated with T4 DNA ligase in a total volume of 150 μl overnight at 16°C, and heated at 65°C for 20 min to inactivate the ligase. The DNA was cleaned by

mixing it with 500 μl of *n*-butanol, pelleting the DNA, and resuspending it in 10 μl water. Finally 2 μl DNA was electrotransformed into *E. coli* strain DH5α λpir, and the electroporated cells were plated on LB agar plates supplemented with kanamycin for selection. Plasmid DNA containing the origin of replication from pMiniHimar-*lacZ* and the flanking myxococcal genomic DNA was prepared using the BIO-RAD Plasmid Miniprep Kit and manufacturer's instructions. The sequence of DNA adjacent to the transposon was obtained using a primer immediately upstream of the right inverted repeat of pMiniHimar-*lacZ* with the sequence 5′-GAA CTA TGT TGA ATA ATA AAA ACG A-3′.

Construction of an in-frame deletion mutant of pglJ *(MXAN2919)*

To create an in-frame deletion, two PCR fragments of 750–800 bp that correspond to the upstream and downstream regions of the target deletion were generated. Primers 5′-CGG AAT TCG GCG CGT GGA CGA AAT CA-3′ and 5′-CGG GAT CCG AGC GCG GAC ACG CTA TC-3′ with restriction sites EcoRI and BamHI, respectively, were used to generate the upstream PCR product. Primers 5′-CGG GAT CCG GGC ACC TGG AGA TGG AA-3′ and 5′-AAC TGC AGC GCC GGC CCA GTC CAT CT-3′ with restriction sites BamHI and PstI, respectively, were used to generate the downstream PCR product. The two PCR products were restriction digested and subcloned into pBJ113 (Table 3) that had been digested with EcoRI and PstI to create the deletion cassette plasmid pRY101 (Table 3). pRY101 was introduced into DK10410 by electroporation as described above. Chromosomal integration of the plasmid was positively selected by mixing recovered transformants with CTT soft agar (0.7% agar) and plated on CTT agar (1.5% agar) supplemented with kanamycin. After 8–10 days of incubation at 32°C, individual kanamycin-resistant colonies were inoculated into 5 ml of fresh CTT medium, and grown to and maintained in exponential phase at 32°C for 3 days. Cells that have lost the vector backbone were negatively selected by plating on CTT agar plates supplemented with 1% galactose. PCR analysis was used to screen cells carrying the in-frame deletion from the ones that carry the wild-type copy. The structure of the in-frame deletion mutant strain DK13024 was confirmed by DNA sequencing.

Analysis of amino acid sequences

Complete CDS were compared with the public protein databases with Protein–Protein BLAST (BLASTP) to seek the possible biochemical function of the protein products by sequence similarity to known proteins (http://www.ncbi.nlm.nih.gov/BLAST/). The Conserved Domain Database (CDD) (http://www.ncbi.nlm.nih.gov/Structure/cdd/cdd.shtml) was also searched.

Visualizing slime

A small amount of exponentially growing *M. xanthus*, suspended in 50 μl of 1/2 CTT medium [0.5% Casitone, 10 mM Tris-HCl (pH 8.0), 8 mM $MgSO_4$, 10 mM KPO_4 (pH 7.6)], was added to a tissue culture well containing 1 ml of 1/2 CTT medium of a 24 well flat bottom plate. After overnight incubation at room temperature in the dark, the tip of a pipette was used to gently scrape the bottom of the culture well and to resuspend the cells that had settled and had moved over the bottom surface of the well. A 3–5 μl droplet of this culture was transferred to a microscope slide and a coverslip was placed on top. Cells and any slime they produced were observed through a 100× DIC objective in a Nikon Eclipse E800 microscope by DIC. Images were collected with a 5 MHz Micromax 5600 cooled CCD camera controlled by Metamorph (Universal Imaging).

Swarm expansion

Swarm expansion was measured using a modified published procedure (Kaiser and Crosby, 1983). *M. xanthus* was grown to exponential phase and concentrated to a calculated density of 2.5×10^9 in CTT medium. An aliquot of 5 μl of each concentrated culture was spotted on plates, prepared the day before use, containing 7 ml of CTT with 1.5% agar in 50×9 mm plastic Petri dishes with tightly fitting lids. After the liquid droplet had soaked into the agar depositing the cells, the plates were closed tightly to prevent further drying and they were incubated at 32°C. Three individual plates were made for each strain. The rate of swarm expansion was quantified by measuring the average width of the zone of spreading, which is the distance between the centre of the swarm and the outermost extents of the swarm. At each time point, two width measurements were made on each of three duplicate swarms. Thus, for each strain, an arithmetic mean of six radius measurements was recorded for that time. The average radius of each strain was plotted against time, and the slope of the resulting line was determined to give the rate of swarm expansion.

Elasticotaxis

The assay for elasticotaxis was performed as previously described (Fontes and Kaiser, 1999) with the following modifications. Square plastic Petri dishes 100×15 mm (Nunc) containing 35 ml of CTT with 1.5% agar were used. A sterile 7-cm-long piece of plastic tubing (3/32 ID, 5/32 OD) was inserted between the dish and the solidified agar to compress the agar by 1 part in 20. Compression squeezed a small amount of liquid from the agar, which was allowed to evaporate at 32°C. The compressed agar was inoculated with 5 μl aliquots of the concentrated (2.5×10^9) *M. xanthus* cultures (prepared as described in *Swarm expansion* section), and incubated at 32°C. At each time point, the diameters of the swarms parallel and perpendicular to the compressing tube were measured, and the ratio between them was calculated to give the coefficient of elasticotaxis (E).

Time-lapse photomicroscopy

M. xanthus strains were grown to exponential phase and diluted to a calculated density of 2.5×10^7 cells ml^{-1} in CTT broth. An aliquot of 5 μl of each diluted culture was spotted on plates containing 7 ml of CTT with 1.5% agarose in

50 × 9 mm plastic Petri dishes (Falcon). After the spot of cells was dried, the plates were incubated at room temperature overnight. A section of the swarm edge was selected and observed under the microscope (Nikon Eclipse E800) by using phase contrast and a 20× objective. Pictures were taken at 30 s intervals for 60–90 min. Images were collected with a SPOT RT SE Monochrome 6 CCD camera (Diagnostic Instruments) controlled through SPOT software. Serial images were saved as QuickTime movies which were examined frame by frame.

For speed measurements, particular cells were chosen from the time-lapse movies that satisfied several criteria: the cell was clearly a single cell and not a group of cells that happened to move as one unit; the cell moved at an approximately constant speed for several frames; the cell had not collided end to end with another cell before the beginning of the selected path; and the cell did not contact any other cell along its path. Using the freehand tool of NIH Image (v1.63) paths of the selected cells were traced and measured to determine the path length in number of pixels. The number of image pixels per micrometer had previously been established from the photograph of a ruled grid of 1/400 m^2. The path measurement was repeated until a consistent value was obtained for both the path of the front of the cell and the path for the back of the same cell. The two values were averaged, and divided by the number of frames spanned by the movement and the time elapsed per frame (30 s) to determine the speed.

To measure the reversal frequency and movement probability, the same procedure was followed except that the strains were grown to a calculated density of 1×10^7 cells ml^{-1} in CTT broth, and an aliquot of 10 μl of each diluted culture was spotted on the plates. After the spot of cells had dried for approximately 30 min, the plates were immediately examined under the microscope. Individual cell movements were tracked over the 120 frames of the 60 min movies manually. Two movies were made for each strain, and approximately 30 individual cells were followed for each movie to determine the number of reversals per hour. For movement probability, starting with the first frame of each QuickTime movie, every cell (roughly 350 cells) was tracked through 15 frames of the movie. Each cell was scored as to whether it moved detectably or not during those 15 frames to obtain the probability of movement during a sample period that represented 12% of the movie.

Acknowledgements

We thank Jonathan Gable for measuring the speed of individual cells. This work was supported by a Postdoctoral Fellowship 5F32GM066649 to R.Y. and a Public health Service Grant GM23441, both from the National Institute of General Medical Sciences.

References

Blackhart, B.D., and Zusman, D. (1985) Frizzy genes of *Myxococcus xanthus* are involved in control of frequency of reversal of gliding motility. *Proc Natl Acad Sci USA* **82:** 8767–8770.

Bourne, H.R., Sanders, D.A., and McCormick, F. (1991) The GTPase superfamily: conserved structure and molecular mechanism. *Nature* **349:** 117–127.

Burchard, R.P. (1981) Gliding motility of prokaryotes: ultrastructure, physiology, and genetics. *Annu Rev Microbiol* **35:** 497–529.

Burchard, R.P. (1982) Trail following by gliding bacteria. *J Bacteriol* **152:** 495–501.

Burchard, R.P. (1984) Gliding motility and taxes. In *Myxobacteria*. Rosenberg, E. (ed.). New York: Springer, pp. 139–161.

Burchard, A.C., Burchard, R.P., and Kloetzel, J.A. (1977) Intracellular periodic structures in the gliding bacterium *Myxococcus xanthus*. *J Bacteriol* **132:** 666–672.

Campbell, J.A., Davies, G.J., Bulone, V., and Henrissaat, B. (1997) A classification of nucleotide-diphospho-sugar glycosyltransferases based on amino acid sequence similarities. *Biochem J* **326:** 929–939.

Cheng, H.-P., and Walker, G.C. (1998) Succinoglycan is required for initiation and elongation of infection threads during nodulation of Alfalfa by *Rhizobium meliloti*. *J Bacteriol* **180:** 5183–5191.

D'Andrea, L.D., and Regan, L. (2003) TPR proteins: the versatile helix. *Trends Biochem Sci* **28:** 655–662.

Fontes, M., and Kaiser, D. (1999) *Myxococcus* cells respond to elastic forces in their substrate. *Proc Nat Acad Sci USA* **96:** 8052–8057.

Hartzell, P., and Kaiser, D. (1991) Upstream gene of the *mgl* operon controls the level of MglA protein in *Myxococcus xanthus*. *J Bacteriol* **173:** 7625–7635.

Henrichsen, J. (1972) Bacterial surface translocation: a survey and a classification. *Bacteriol Rev* **36:** 478–503.

Hodgkin, J., and Kaiser, D. (1977) Cell-to-cell stimulation of movement in nonmotile mutants of *Myxococcus*. *Proc Natl Acad Sci USA* **74:** 2938–2942.

Hodgkin, J., and Kaiser, D. (1979a) Genetics of gliding motility in *M. xanthus* (Myxobacterales): two gene systems control movement. *Mol Gen Genet* **171:** 177–191.

Hodgkin, J., and Kaiser, D. (1979b) Genetics of gliding motility in *M. xanthus* (Myxobacterales): genes controlling movement of single cells. *Mol Gen Genet* **171:** 167–176.

Hoiczyk, E., and Baumeister, W. (1998) The junctional pore complex, a prokaryotic secretion organelle, is the molecular motor underlying gliding motility in cyanobacteria. *Current Biol* **8:** 1161–1168.

Jahn, E. (1924) *Beitrage Zur Botanischen Protistologie. I. Die Polyangiden.* Leipzig: Gebruder Borntraeger.

Jelsbak, L., and Søgaard-Andersen, L. (1999) The cell-surface associated C-signal induces behavioral changes in individual *M. xanthus* cells during fruiting body morphogenesis. *Proc Nat Acad Sci USA* **96:** 5031–5036.

Julien, B., Kaiser, A.D., and Garza, A. (2000) Spatial control of cell differentiation in *Myxococcus xanthus*. *Proc Nat Acad Sci USA* **97:** 9098–9103.

Kaiser, A.D. (1979) Social gliding is correlated with the presence of pili in *Myxococcus xanthus*. *Proc Natl Acad Sci* **76:** 5952–5956.

Kaiser, A.D. (2007) Reversing *M. xanthus* polarity. In *Multicellularity and Differentiation among the Myxobacteria and Their Neighbors*. Kaplan, H.B., and Whitworth, D. (eds).

Washington, DC: American Society for Microbiology Press, Ch. 5.

Kaiser, A.D., and Crosby, C. (1983) Cell movement and its coordination in swarms of *Myxococcus xanthus*. *Cell Motility* **3:** 227–245.

Kaiser, D. (2003) Coupling cell movement to multicellular development in myxobacteria. *Nature Rev Microbiol* **1:** 45–54.

Kaiser, D., and Yu, R. (2005) Reversing cell polarity: evidence and hypothesis. *Cur Opin Microbiol* **8:** 216–221.

Kuhlwein, H., and Reichenbach, H. (1968) *Swarming and Morphogenesis in Myxobacteria.* Gottingen, Ger: Institute Wissensch. Film.

Lapidus, I.R., and Berg, H. (1982) Gliding motility of Cytophaga sp. strain U67. *J Bacteriol* **151:** 384–398.

Lunsdorf, H., and Schairer, H.U. (2001) Frozen motion of gliding bacteria outlines inherent features of the motility apparatus. *Microbiology* **147:** 939–947.

McBride, M.J. (2000) Bacterial gliding motility: mechanisms and mysteries. *ASM News* **66:** 203–210.

McBride, M.J.M. (2001) Bacterial gliding motility: multiple mechanisms for cell movement over surfaces. *Annu Rev Microbiol* **55:** 49–75.

Nudleman, E., and Kaiser, D. (2004) Pulling together with type IV pili. *J Mol Microbiol Biotechnol* **7:** 52–62.

Nudleman, E., Wall, D., and Kaiser, D. (2005) Cell-to-cell transfer of bacterial outer-membrane lipoproteins. *Science* **309:** 125–127.

Nudleman, E., Wall, D., and Kaiser, D. (2006) Polar assembly of the type IV pilus secretin in *Myxococcus xanthus*. *Mol Microbiol* **60:** 16–29.

Pate, J.L., Chang, L.-Y.E. (1979) Evidence that gliding motility in prokaryotic cells is driven by rotary assemblies in the cell envelopes. *Curr Microbiol* **2:** 59–64.

Raetz, C.R.H., and Whitfield, C. (2002) Lipopolysaccharide endotoxins. *Annu Rev Biochem* **71:** 635–700.

Reed, J.W., and Walker, G.C. (1991) The *exoD* gene of *Rhizobium meliloti* encodes a novel function needed for alfalfa nodule invasion. *J Bacteriol* **173:** 664–677.

Reichenbach, H., Heunert, H.H., and Kuczka, H. (1965) *Myxococcus Spp. (Myxobacteriales) Schwarmentwicklung und Bildung Von Protocysten. Film E778.* Gottingen, Ger: Institute Wissensch. Film.

Rodriguez, A.M., and Spormann, A.M. (1999) Genetic and molecular analysis of *cglB*, a gene essential for single-cell gliding in *Myxococcus xanthus*. *J Bacteriol* **181:** 4381–4390.

Simunovic, V., Gherardini, F.C., and Shimkets, L.J. (2003) Membrane localization of motility, signaling, and polyketide synthase proteins in *Myxococcus xanthus*. *J Bacteriol* **185:** 5066–5075.

Spormann, A.M., and Kaiser, D. (1999) Gliding mutants of *Myxococcus xanthus* with high reversal frequencies and small displacements. *J Bacteriol* **181:** 2593–2601.

Stanier, R.Y. (1942) Elasticotaxis in myxobacteria. *J Bacteriol* **44:** 405–412.

Stephens, K., and Kaiser, D. (1987) Genetics of gliding motility in *Myxococcus xanthus*: molecular cloning of the *mgl* locus. *Mol Gen Genet* **207:** 256–266.

Stephens, K., Hartzell, P., and Kaiser, D. (1989) Gliding motility in *Myxococcus xanthus*: the *mgl* locus, its RNA and predicted protein products. *J Bacteriol* **171:** 819–830.

Vale, R.D. (2000) AAA proteins: lords of the ring. *J Cell Biol* **150:** F13–F19.

Wall, D., Kolenbrander, P.E., and Kaiser, D. (1999) The *Myxococcux xanthus pilQ* (*sglA*) gene encodes a secretin homolog required for type IV pili biogenesis, S motility and development. *J Bacteriol* **181:** 24–33.

Ward, M.J., Lew, H., Treuner-Lange, A., and Zusman, D.R. (1998) Regulation of motility behavior in *Myxococcus xanthus* may require an extracytoplasmic-function sigma factor. *J Bacteriol* **180:** 5668–5675.

White, D.J., and Hartzell, P.L. (2000) AglU, a protein required for gliding motility and spore maturation of *Myxococcus xanthus*, is related to WD-repeat proteins. *Mol Microbiol* **36:** 662–678.

Whitfield, C., and Roberts, I.S. (1999) Structure, assembly and regulation of expression of capsules in *Escherichia coli*. *Mol Microbiol* **31:** 1307–1319.

Wolgemuth, C. (2005) Force and flexibility of flailing myxobacteria. *Biophys J* **89:** 1643–1649.

Wolgemuth, C., Hoiczyk, E., Kaiser, D., and Oster, G. (2002) How myxobacteria glide. *Current Biology* **12:** 369–377.

Wu, S.S., and Kaiser, D. (1997) Regulation of expression of the *pilA* gene in *Myxococcus xanthus*. *J Bacteriol* **179:** 7748–7758.

Youderian, P., Burke, N., White, D.J., and Hartzell, P.L. (2003) Identification of genes required for adventurous gliding motility in *Myxococcus xanthus* with the transposable element mariner. *Mol Microbiol* **49:** 555–570.

